



Can Climate Models Simulate the Observed Strong Summer Surface Cooling in the Equatorial Atlantic?

Tina Dippe, Martin Krebs, Jan Harlaß,
and Joke F. Lübbecke

Abstract

Variability in the tropical Atlantic Ocean is dominated by the seasonal cycle. A defining feature is the migration of the inter-tropical convergence zone into the northern hemisphere and the formation of a so-called cold tongue in sea surface temperatures (SSTs) in late boreal spring. Between April and August, cooling leads to a drop in SSTs of approximately 5° . The pronounced seasonal cycle in the equatorial Atlantic affects surrounding continents, and even minor deviations from it can have striking consequences for local agricultures.

Here, we report how state-of-the-art coupled global climate models (CGCMs) still struggle to simulate the observed seasonal cycle in the equatorial Atlantic, focusing on the formation of the cold tongue. We review the basic processes that establish the observed seasonal cycle in the tropical Atlantic, highlight common biases and their potential origins, and discuss how they relate to the dynamics of the real world. We also briefly discuss the implications of the equatorial Atlantic warm bias for CGCM-based reliable, socio-economically relevant seasonal predictions in the region.

The Equatorial Atlantic: A Climate Hot Spot

The tropical oceans are a crucial element of the global climate system. Defined here as the ocean area between 15°N and 15°S , they occupy only about 13% of the earth's surface, but receive approximately 30% of the global net surface insolation.¹ Processes both in the ocean and the atmosphere redistribute surplus heat from low to higher latitudes. Without these mechanisms, the tropics would get steadily warmer, while the polar regions would radiate away more heat than they receive and hence continue to cool. The oceans help to establish the overall radiative equilibrium that is responsible for our relatively stable climate (Trenberth and Caron 2001).

Apart from the energy surplus, another defining feature of an equatorial ocean is that the effect of the earth's rotation vanishes at the equator, giving rise to a physical framework that is subtly different from its higher-latitude counterpart. The effect of the earth's rotation manifests in a pseudo-force that is called the Coriolis force. It deflects large-scale motion towards the right of the movement on the northern hemisphere and towards the left on the southern hemisphere. It provides rotation to large weather systems and explains why large-scale movement curves or even becomes circular. An exception is the equator, where the Coriolis force vanishes and movement can be straightforward. Additionally, the non-existent Coriolis force at the equator acts as a barrier for the transmission of information within the ocean, for example

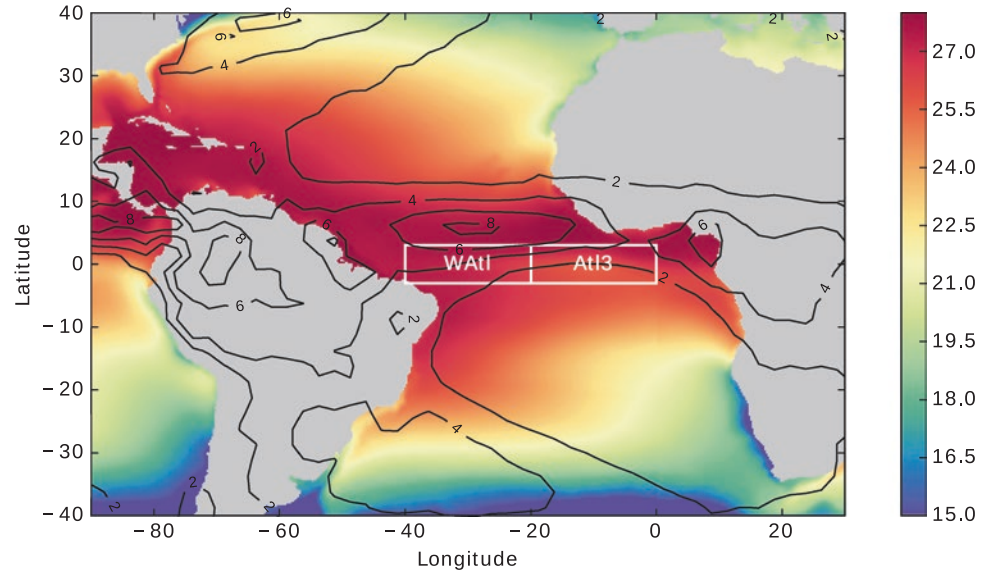
¹Based on data by Trenberth et al. (2009).

T. Dippe (✉) · M. Krebs · J. Harlaß
GEOMAR Helmholtz Centre for Ocean Research Kiel,
Kiel, Germany
e-mail: tdippe@geomar.de; jharlass@geomar.de

J. F. Lübbecke
GEOMAR Helmholtz Centre for Ocean Research Kiel,
Kiel, Germany

Faculty of Mathematics and Natural Sciences, Christian Albrechts
University, Kiel, Germany
e-mail: jluebbecke@geomar.de

Fig. 1 The observed tropical Atlantic mean state sea surface temperature (SST) and precipitation: Annual mean sea surface temperatures are shown as shading, precipitation in contours. White boxes indicate the Atl3 and WAtl region in the eastern and western tropical Atlantic, respectively. The used datasets are the NOAA Optimum Interpolated SST dataset (OISST, Reynolds et al. 2007; Banzon et al. 2016), and the NOAA Climate Prediction Center (CPC) Merged Analysis of Precipitation dataset. (CMAP, Xie and Arkin 1997)



via equatorial Kelvin waves. Communicating information from the southern to the northern hemisphere and vice versa is hence a non-trivial enterprise in the ocean.

While the basic set-up of the marine tropical climate system is identical in all three tropical oceans, details differ between basins. The Pacific Ocean has the largest extent and is characterized by a relatively simple land-ocean geometry; it behaves much like a perfect theoretical ocean. The tropical Atlantic, in contrast, is much narrower and the surrounding continents interact with the ocean in complex ways. For example, the tropical Atlantic appears to be more susceptible to extra-equatorial influences (e.g., Foltz and McPhaden 2010; Richter et al. 2013; Lübbecke et al. 2014; Nnamchi et al. 2016), and variability is due to a number of interacting mechanisms on overlapping time scales (Sutton et al. 2000; Xie and Carton 2004). Therefore, the tropical Atlantic is less readily understood than the tropical Pacific, and still poses substantial challenges to the scientific community.

The mean state of the tropical Atlantic is characterized by a complex interplay of atmospheric and oceanic features. These are i) the trade wind systems of both the northern and southern hemispheres, ii) a system of alternating shallow zonal² currents in the ocean, and iii) a zonal gradient in upper-ocean heat content that is also reflected in a pronounced zonal gradient in sea surface temperatures (SSTs), with warm temperatures in the west and cooler surface waters in the east. Figure 1 illustrates the mean state of SST and precipitation.

The trade winds are part of the climate system’s hemispheric response to the strong temperature gradient between the polar and the equatorial regions. Intense (solar) surface

heating at the equator produces warm and humid, ascending air masses. During the ascend, part of the air moisture condensates and releases latent heat, which further accelerates the rising motion. The upward flow moves mass from the surface layer towards the top of the troposphere, effectively decreasing surface pressure and forming a low-pressure trough. At the surface, a compensation flow towards the low-pressure trough is established. Due to the rotation of the earth, however, the flow veers to the west and creates the surface trade winds. The northeasterly and southeasterly trade winds of the northern and southern hemispheres, respectively, converge in the inter-tropical convergence zone (ITCZ), a zonal band of intense precipitation and almost vanishing horizontal winds (Fig. 1). Because the ITCZ is located to the north of the equator in the Atlantic, the equatorial Atlantic is not dominated by the ITCZ itself, but by the trade wind system of the southern hemisphere that provides relatively steady easterly winds on the equator. (See below for why the ITCZ is, on average, not residing on the equator in the tropical Atlantic.)

A consequence of the easterly wind forcing at the ocean surface and the vanishing Coriolis force at the equator is that the wind pushes the warm surface waters westward. Water piles up to the east of Brazil in the Atlantic warm pool, providing water temperatures of approximately 28 °C at the surface. Conversely, the surface layer of warm water in the eastern tropical Atlantic is thinned out considerably – the eastern part of the basin stores much less heat in the upper ocean than the western part. A pronounced zonal gradient in upper-ocean heat content is established. Figure 8a illustrates this mean state.

The pressure below the ocean surface is not uniform across the basin either. At the equator, the bulk of warm water in the western ocean basin adds pressure to the water

²“Zonal” refers to an east-west orientation, i.e. one that is parallel to the equator. A north-south orientation is called “meridional”.

Divergence-driven upwelling

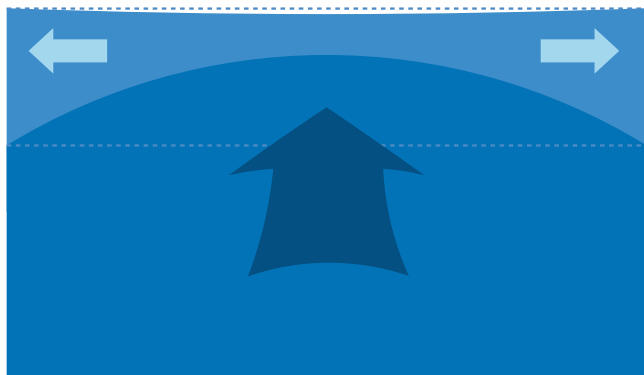


Fig. 2 Upwelling driven by horizontal divergence. Consider an ocean in a state of rest. In a simple model, a layer of warm water is sitting on top of a layer of colder water. Both the interfaces between the warm surface layer and the atmosphere, and between the colder subsurface water and surface layer are approximately even (horizontal dashed blue lines). When a divergence is created in the upper layer, mass is transported away from the divergence (light blue arrows in the surface layer). Because water is approximately incompressible, mass must be conserved. A vertical flow from the subsurface layer compensates the horizontal divergence (dark blue, upward arrow). In reality, this domes the interface between the surface and the subsurface layers. The sea surface adapts to the doming interface by decreasing in a similar fashion, albeit with a much smaller amplitude

column, while eastern ocean pressure is reduced. The resulting east-west pressure gradient is balanced by a strong eastward current right below the surface – the equatorial undercurrent (EUC) (Cromwell 1953; Cromwell et al. 1954). At the surface, on the other hand, the direct wind forcing and meridional pressure gradients produce a complex system of alternating zonal current bands (e.g., Schott et al. 2003; Brandt et al. 2006, 2008).

The three-dimensional flow of the upper equatorial oceans directly below the well-mixed surface layer is characterized by a slow but steady upward motion of, at best, a few meters per day (Rhein et al. 2010). This so-called “upwelling” is maintained by two processes. First, the Coriolis force deflects the off-equatorial components of the wind-induced westward displacement of surface water masses into opposite directions. On the northern hemisphere, westward flow veers north, while the Coriolis force directs it south on the southern hemisphere. Zonal wind-driven upper ocean mass transports diverge; they effectively transport mass away from the equator. However, because mass is conserved, sea level sags imperceptibly, and upwelling transports colder, subsurface water closer to the surface by creating a “dome” in the interface between the warm surface water and cooler subsurface water. The ratio between the surface and subsurface layer thicknesses changes in response to the surface divergence. Figure 2 illustrates how divergent flow in the surface layer creates upwelling and changes the geometry of the involved

interfaces between both the atmosphere and the ocean, and the ocean surface and subsurface layers.

Second, a small meridional contribution to the equatorial wind field contributes to maintaining equatorial upwelling. These meridional contributions are illustrated in Fig. 7b by the equatorial wind vectors that do not point straight to the west but rather to the northwest, as they are part of the southern hemisphere trade wind regime crossing the equator into the northern hemisphere for most of the year. In the ocean, they induce meridional surface mass transports slightly off the equator (Philander and Pacanowski 1981). Again, the Coriolis force redirects these meridional motions into zonal mass transports of opposite signs, which contribute to the upper ocean horizontal divergence.

Over the course of the year, the set-up of this basic state varies. Due to the tilted rotational axis of the earth, the latitude of maximum insolation shifts into the northern hemisphere in boreal – i.e. northern hemispheric – summer, and into the southern hemisphere in boreal winter. The ITCZ, accompanied by the trade wind systems of both hemispheres, migrates in a similar fashion. However, the ITCZ does not oscillate around the equator but stays north of it for most of the year (Hastenrath 1991; Mitchell and Wallace 1992). Xie (2004) reviewed the “riddle” of the asymmetric ITCZ and concluded that it is, contrary to intuition, not so much the overall distribution of landmasses and oceans that anchors the Atlantic ITCZ to the northern hemisphere, but a combination of air-sea coupling and the shape of the West-African shoreline. More recently, Frierson et al. (2013) also demonstrated how the meridional temperature gradient between the warm northern hemisphere and the relatively colder southern hemisphere impacts the ITCZ behavior. All factors combine to pull the trade wind system of the southern hemisphere across the equator and establish the highest SSTs to the north of the equator.

Driven by the changing trade wind systems, the zonal surface current systems vary in strength and location. The intensity of the Equatorial Undercurrent, while firmly pinned to the equator, varies as well (Johns et al. 2014). Variations in the wind forcing lead to seasonally recurring intensifications of the zonal heat content gradient.

One of the most striking elements of the tropical Atlantic seasonal cycle is the formation of the Atlantic cold tongue in the eastern equatorial Atlantic during boreal summer. The cold tongue is characterized by an intense cooling of the upper ocean. Figure 3a shows that SSTs in the Atl3 region (3°S – 3°N , 20°W – 0°E) drop from 28°C to about 23°C between April and August, forming a distinct, tongue-shaped pattern of relatively cool surface water that stretches from the West African coast into the central equatorial Atlantic (Figs. 3b, c). The observed temperature difference between April and August in the upper 50 m of the Atl3 region alone corresponds to a change in thermal energy of

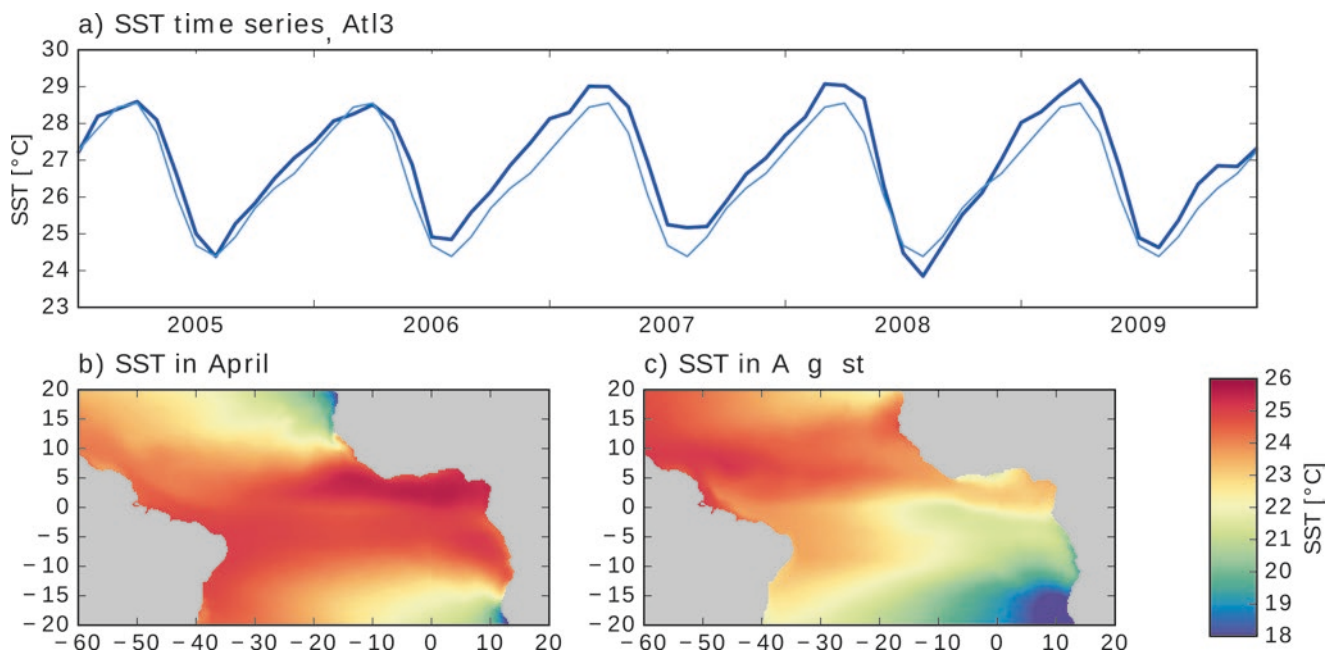


Fig. 3 Observed cold tongue based on the NOAA Optimum Interpolated SST dataset (OISST). (a) Exemplary time series of monthly mean Atl3 sea surface temperature (SST, dark blue) and the climatological seasonal cycle (light blue). For the seasonal cycle,

monthly mean data has been averaged for each calendar month for the period 1981–2012. (b) and (c) Climatological SST fields for April and August, illustrating the climatological conditions when SSTs reach their maximum just before the onset of the cold tongue, and when the cold tongue is fully developed, respectively

1351.16 EJ.³ That is 13 times the US-American energy consumption of 2014, or 2.6 times the total global energy consumption of 2011.

The formation of the cold tongue co-occurs with seasonal changes in the atmospheric circulation. An important and well-known aspect of this is the strong co-variability between the onset of the cold tongue and the onset of the West African monsoon (e.g., Okumura and Xie 2004; Brandt et al. 2011a; Caniaux et al. 2011), a key element of large-scale precipitation in western Africa and hence a crucial factor of agriculture. Understanding the complex processes that shape the coupled atmosphere-ocean-land climate system of the equatorial Atlantic is a task of high societal relevance.

In concert with accurate and long-term observations, climate models are an essential tool to investigate the equatorial Atlantic. Here we address the question of how well state-of-the-art climate models are able to reproduce the observed seasonal cycle of the equatorial Atlantic. The section “Climate models: A crash course” gives an overview on coupled climate models and introduces the concept of model biases. The section “Can climate models reproduce the observed seasonality of the equatorial Atlantic climate system?” reports common biases in the tropical Atlantic and how they relate to the formation of the modeled cold tongue.

³Based on thermal data from the World Ocean Atlas (WOA2013v2, Locarnini et al. 2013).

An outlook in the last section addresses the usefulness of climate models for studies of cold tongue variability, a crucial source of tropical Atlantic climate variability that strongly affects the surrounding continents.

Climate Models: A Crash Course

Climate models numerically solve the Navier-Stokes equations for a set of specified assumptions. The Navier-Stokes equations are a system of non-linear partial differential equations that describe the behavior of fluids, from a drop of water that hits the surface of a puddle, to global circulation systems such as the trade wind systems. They are highly complex and can only be solved numerically when they are approximated to focus on a specific class of fluid processes. For climate models, these processes are mostly related to the large-scale global circulation, synoptic phenomena, and possibly mesoscale phenomena⁴ such as ocean eddies. The approximated Navier-Stokes equations that are used in current climate models are called the primitive equations.

Climate models consist of a number of “building blocks”. The two core building blocks are an atmosphere and an ocean general circulation model (GCM). Given appropriate surface and boundary forcing, both GCM types can be run

⁴Size on the order of 10–50 km.

independently. Phillips (1956) demonstrated this by designing the first successful atmospheric GCM. To allow the oceanic and atmospheric blocks to interact with each other, a coupling module exchanges information at the air-sea interface. A coupler and the atmospheric and oceanic GCMs together form the simplest coupled GCM (CGCM). Such a basic CGCM lacks a number of relevant processes, relating for example to the land and sea ice components of the climate system or the impact of vegetation. To introduce these important aspects into the model, CGCMs are “upgraded” with additional building blocks to form earth system models. If a basic CGCM is a simple brick house of only one room, a full-fledged earth system model is a mansion with specialized rooms for different tasks. Important additional building blocks for an earth system model are modules that simulate the behavior of sea ice, ice sheets and snow cover on land, vegetation and other surface processes such as river runoff into the ocean, atmospheric chemistry, biogeochemistry in the ocean or even geological processes of varying complexity.

In order to solve the model equations numerically, CGCMs need to discretize the real world into finite spatial and temporal units. The basis for such a discretization is a three-dimensional grid of grid boxes that each contain a single value of a given variable. The CGCM applies the model equations to the grid boxes and integrates them forward in time. Essentially, each grid box is a mini-model that is, however, exchanging information with neighboring grid boxes.

An important characteristic of a model grid is its resolution, i.e. the size of its grid boxes.⁵ It defines, among other things, which processes can be resolved. As an example, consider the development of cumulus clouds. While cumulus clouds have a horizontal scale of less than 10 km, state-of-the-art models use a resolution of about 100 km. On such a grid CGCMs cannot simulate cumulus clouds directly. Consequently, the climatic impacts of such clouds have to be parameterized, i.e. their effect must be captured by the model in a simpler way that is supported by observations. For convective⁶ and mixing processes alone – important aspects of cumulus clouds –, a number of parameterization schemes exist that subtly alter the behavior of large-scale processes in the models.

In addition to horizontal processes, models must be able to capture vertical motions in the climate system. Cumulus clouds, for example, extend vertically throughout varying

portions of the troposphere, and vertical movement within clouds is a key factor of precipitation. On a larger scale, ascending air masses within the ITCZ define an important aspect of the tropical climate system (cf. Section “[The equatorial atlantic: A climate hot spot](#)”). Models need to be able to reproduce these vertical movements. They require vertical layering, giving rise to the three-dimensional structure of a model grid. A common feature of all models is that their vertical levels are unevenly distributed. Because properties usually change drastically close to the air-sea interface, resolving these strong gradients requires a high vertical resolution. Conversely, the thickest levels are farthest away from the air-sea interface. In the ocean, the last model level usually ends at the sea floor; the atmosphere, however, is not bounded that clearly. Some models only resolve the troposphere, our “weather” sphere that reaches up to approximately 15 km, while a number of recent atmosphere models incorporate the stratosphere as well (up to 80 km).

Figure 4 illustrates schematically how the different “building blocks” of a CGCM work together and how the real world must be discretized into grid boxes to allow a numerical solution of the primitive equations.

CGCMs are initialized either from a state of rest – i.e. the ocean and atmosphere are without motion and only establish their general circulation patterns during the first stage of the simulation, the so-called “spin-up” – or from a more specific state that is generally derived from observations. In both cases, the model needs time to smooth out initial imbalances and establish an equilibrium. Additionally, climatically relevant forcing parameters must be prescribed to the model in the form of boundary conditions. A prominent example of such a boundary condition is the strength and variability of the solar forcing, our energy source on earth, or the atmospheric CO₂ concentration.

Climate models are used to address a host of research questions. They aid scientists in interpreting observations, infer mechanisms, or provide information on how the climate system might evolve in the future. All of these tasks, however, require that CGCMs are able to produce a realistic climate. Due to various limitations, this is not always the case. A common manifestation of the shortcomings of a climate model is the formation of biases.

A bias is a systematic difference between the modeled and the observed climate. This difference can occur in any statistical property of any model variable. While standard biases are routinely monitored during the development and application of climate models, non-obvious biases may be present in simulations that look fine otherwise. Consider, for example, SST in a given location. While routine bias controls may have found a realistic mean SST, closer inspection could reveal that SST anomalies tend to be too high. Because positive and negative anomalies cancel each other out on

⁵Note that, usually, not all grid boxes of a GCM have the same size, neither in terms of absolute surface area, nor in terms of longitudinal and latitudinal extent. A common practice in ocean models, for example, is to refine the latitudinal resolution towards the equator to better resolve the fine structures of the equatorial oceans. In a similar fashion, Sein et al. (2016) recently discussed grid layouts for ocean models that increase their spatial resolution in certain target areas.

⁶Convection: upward motion in the atmosphere.

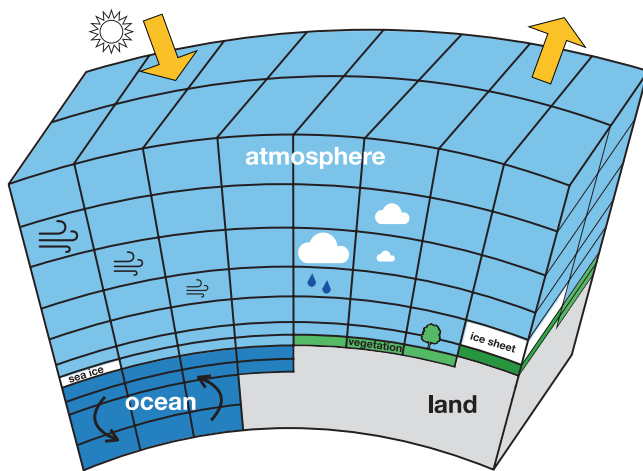


Fig. 4 Schematic of a Coupled General Circulation Model (CGCM). On the most basic level, the earth is a closed system that receives energy from the sun and radiates away thermal energy (yellow arrows at the “top of the atmosphere”). A CGCM tries to simulate the processes within this system. It consists of a number of modules that interact with each other. Important modules in state-of-the-art CGCMs are the ocean-and-sea-ice module, the atmospheric module, and additional modules that simulate, for example, land surface processes or vegetation. These “building blocks” of the CGCM exchange information with each other via an additional “coupling module”. Coupling is a computationally expensive operation that can account for up to a third of the total required computational resources of a CGCM. A CGCM solves an approximation to the Navier-Stokes equations numerically. These are a set of non-linear partial differential equations that describe the motion of fluids. To solve them, the model must discretize the real world into finite spatial and temporal units. In the three-dimensional space domain, this discretization results in a layered grid. Each grid box contains a single value for each model variable. Processes acting on spatial scales that are smaller than the extent of the grid box must be parameterized. Prominent examples of these “sub-grid” processes are, for example, the formation of clouds and precipitation

average, this biased variance would not be obvious. In a similar manner, positive and negative SST anomalies might not be distributed realistically, with the model perhaps producing a few very strong positive anomalies and many weak negative anomalies that still form the expected average. In this case, the modeled SST distribution is skewed with respect to observations.

An additional limitation on the hunt for biases is that a bias can only be diagnosed in comparison to a reliable observational benchmark. Many parameters of the real climate system, however, are hard to observe or have only been observed for a short time. In general, large-scale patterns on the earth’s surface and throughout the atmosphere can be observed relatively easily with satellite-borne remote sensing instruments. SST, for example, has been carefully monitored by a number of satellite missions since the 1980s. Processes below the ocean surface, however, can usually not be monitored from space. Instead, observational data have to be obtained by measurements from ships, moored instruments and autonomous vehicles such as gliders and floats.

For the tropical oceans, the TAO/TRITON mooring array in the Pacific (McPhaden 1995), the PIRATA array in the Atlantic (Bourlès et al. 2008), and the RAMA array in the Indian Ocean (McPhaden et al. 2009) provide, among others, information on temperature, salinity, current velocities and air-sea fluxes. Additionally, an increasing number of hydrographic observations have become available over the last decade due to the Argo program (Roemmich et al. 2009). While all of these measurements provide invaluable information about the state of the tropical oceans, they are not spatially continuous and have only been operational for the last few decades. Obtaining information about the evolution of the climate system in the past remains a core challenge of climate research.

Although no climate model is exactly like the other, some biases are shared by a wide range of state-of-the-art CGCMs. Figure 5 shows the global pattern of the annual mean SST bias for the average of 33 CGCMs and an experiment with the Kiel Climate Model (KCM, Park et al. 2009). Positive values indicate that modeled SST is warmer than in observations and vice versa. We validated the performance of these CGCMs and the KCM in terms of SST against the satellite derived Optimum Interpolated SST dataset (OISST, Reynolds et al. 2007; Banzon et al. 2016). Figure 5 shows that while the KCM is a unique model that has individual flaws and strengths, the characteristics of its equatorial Atlantic SST bias are well comparable to other current CGCMs (examples of other models are shown, among others, in Wahl et al. 2011; Xu et al. 2014; Ding et al. 2015; Harlaß et al. 2017).

The KCM is a state-of-the-art CGCM that was integrated with radiative forcing for the period 1981–2012 in rather coarse resolution. The ocean-sea ice model NEMO (Madec 2008) was run with 31 vertical levels and a horizontal resolution of 2° that is refined to 0.5° in the equatorial region. The atmospheric model ECHAM5 (Roeckner et al. 2003) is run with 19 vertical levels and a global horizontal resolution of approximately 3.75° . Results from KCM simulations are selected here for consistency reasons. We stress again that while the KCM differs wildly from other CGCMs in some aspects, its simulation of the tropical Atlantic is representative for most current-generation CGCMs.

Can Climate Models Reproduce the Observed Seasonality of the Equatorial Atlantic Climate System?

The Equatorial Atlantic Warm Bias: Symptoms

The annual mean SST bias varies considerably between different regions of the ocean (Fig. 5). Striking features of the global SST bias pattern are the pronounced warm biases

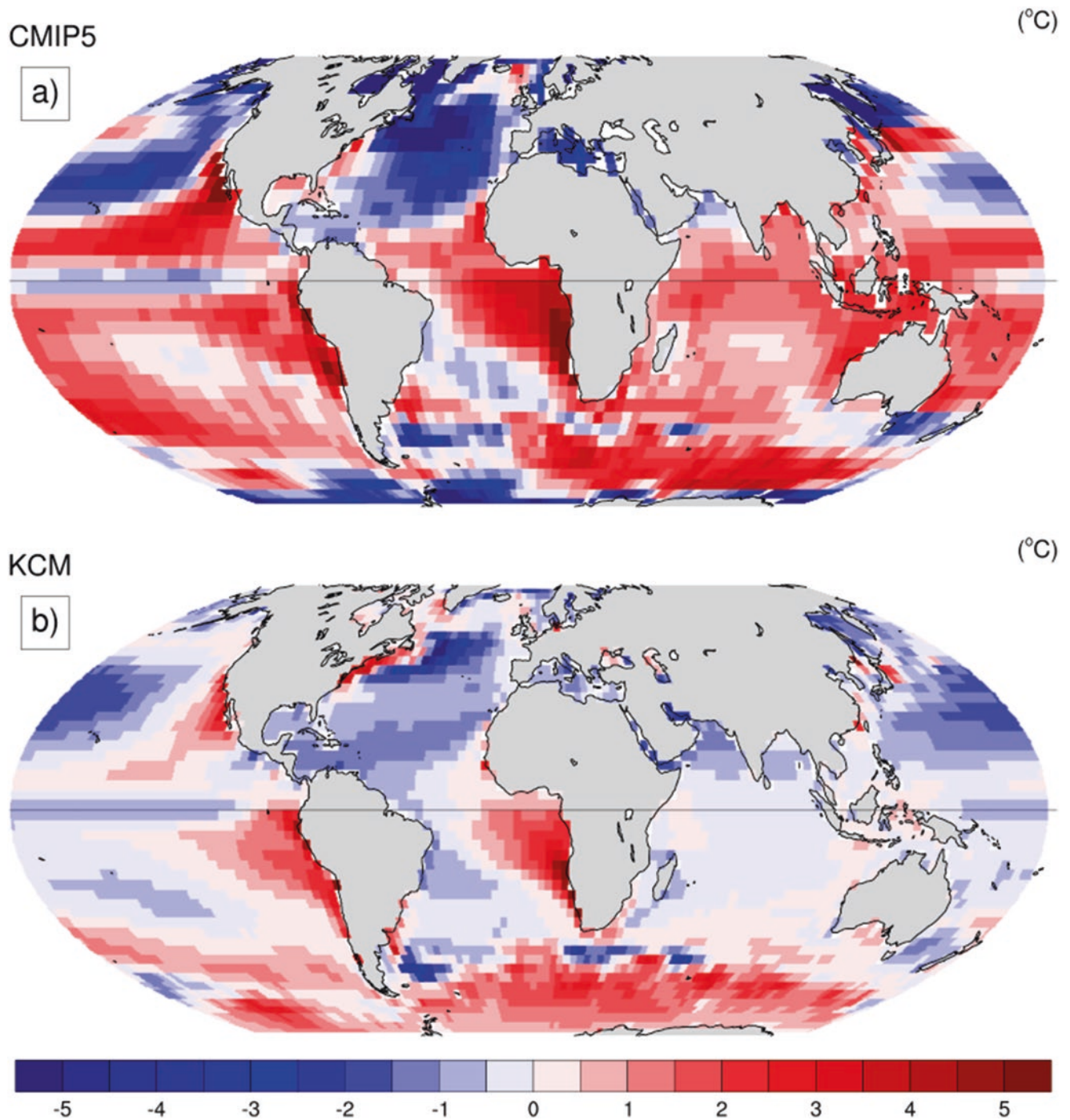
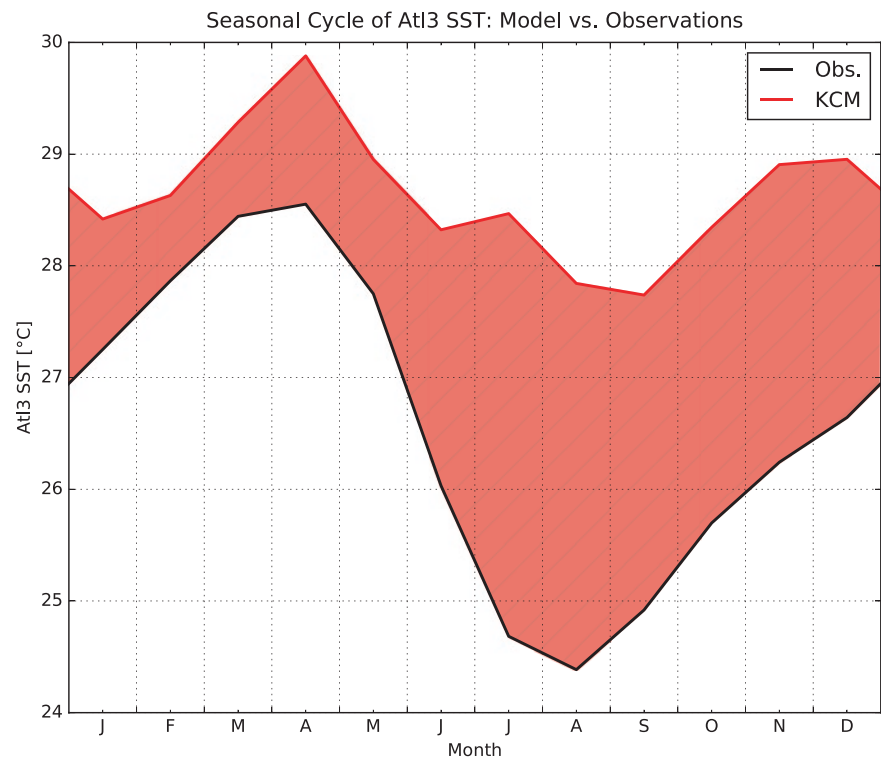


Fig. 5 Annual mean global sea surface temperature (SST) bias in (a) the ensemble mean of 33 Coupled General Circulation Models (CGCMs) contributing to the Coupled Model Intercomparison Project, Phase 5 (CMIP5, Taylor et al. 2012) and (b) one integration of the Kiel Climate Model (KCM). For CMIP5, the chosen experiments were “historical” experiments that were forced by the observed changes in atmospheric composition. The KCM was run with an atmospheric horizontal resolution of approximately 3.75° and with 19 vertical levels. The

ocean model had a horizontal resolution of 2° that was refined to 0.5° towards the equator, and 31 vertical levels. The annual mean SST bias was diagnosed with respect to the NOAA Optimum Interpolated SST dataset (OISST) for the period 1982–2009. Using an ensemble mean of three ensembles instead of a single integration to diagnose the KCM SST bias changed the results only negligibly. This demonstrates how robust a feature the annual mean SST bias pattern is in the KCM

Fig. 6 Seasonal cycle of Atl3 sea surface temperature (SST) in observations (NOAA Optimum Interpolated SST dataset, black), and the Kiel Climate Model (KCM, red). Red shading illustrates the bias magnitude for each month



along the subtropical western shorelines of all continents. These biases appear, for example, along the western US-American as well as the Peruvian and Chilean coasts in the Pacific, or off Angola and Namibia in the Atlantic. They are anchored to the eastern boundary upwelling systems, where cold subsurface waters are brought close to the ocean surface. Here, SST biases can reach annual mean amplitudes of up to 7 °C in current climate models (Xu et al. 2014).

In this section, we focus on the pronounced warm bias that covers the equatorial Atlantic cold tongue region. The annual mean SST bias in the Atl3 region has a magnitude of approximately 2 °C.⁷ In the upper 50 m of Atl3 in the KCM, this corresponds to a heat surplus of approximately 380 EJ, an amount of energy that could melt 47 times the ice volume of the Antarctic ice sheet.⁸

An important aspect of the equatorial Atlantic SST bias is that it varies over the course of the year. Figure 6 shows that the SST bias of the KCM is smallest in boreal winter, with a value of less than 1 °C in February. During the cold tongue formation, it rapidly increases to almost 4 °C until July. For the rest of the year, it slowly decreases again. This implies

⁷Note, however, that by no means *all* climate models develop such a strong equatorial Atlantic warm bias. Some models are capable of simulating a more realistic tropical Atlantic, but these models represent but a tiny minority of all current CGCMs.

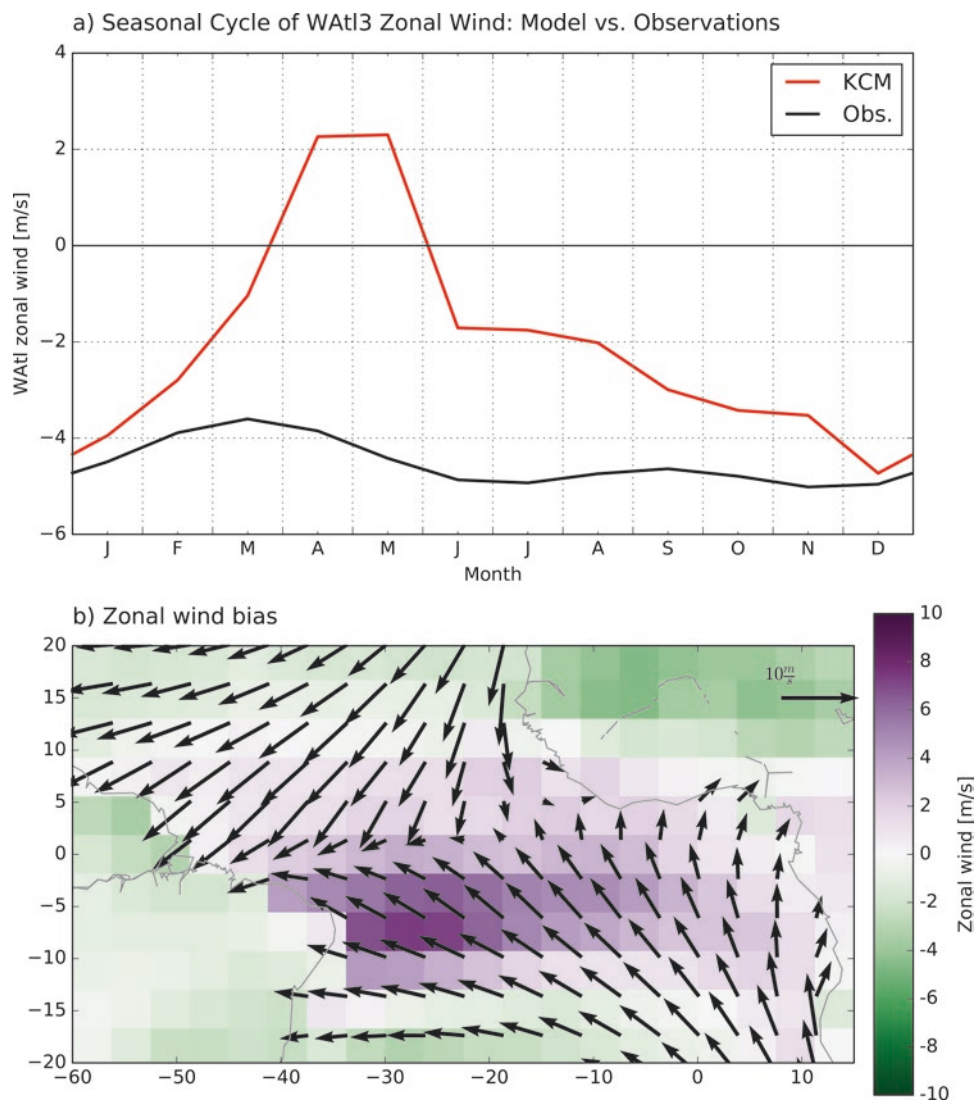
⁸We used the thermal data from WOA2013v2 to compare our model results with. The Antarctic ice volume is based on the Bedmap2 dataset (Fretwell et al. 2013).

that the KCM struggles to simulate the observed strong cooling that is associated with the development of the cold tongue in boreal summer. Indeed, Fig. 6 shows that the KCM – similar to most state-of-the-art CGCMs (e.g., Richter and Xie 2008; Richter et al. 2014b) – does not produce a coherent cold tongue that is comparable in strength to observations. A key process of the equatorial Atlantic climate system is missing from the simulations.

Because the ocean and the atmosphere are strongly coupled in the tropics, the missing cold tongue is only one symptom of a fundamentally biased equatorial Atlantic in current climate models. Figure 7 illustrates the bias of the zonal wind component in the KCM. During spring, the KCM strongly underestimates the magnitude of zonal wind in the western tropical Atlantic (Fig. 7a). While the absolute value of zonal wind is higher in the KCM than in observations, especially during spring, the magnitude is much smaller. Instead of the generally easterly winds (negative values), associated with the trade winds, the KCM simulates very weak westerly winds (positive values). This “westerly wind bias” – so-called because the simulated zonal winds are much too westerly compared to the observed trade winds – is another typical bias pattern in state-of-the-art GCMs. It agrees with an ITCZ that is displaced too far to the south, a feature that is common to both coupled and atmosphere-only GCMs (e.g., Doi et al. 2012; Richter et al. 2012; Siongco et al. 2015).

An important question is: How do the different bias symptoms relate to each other dynamically, and how do these

Fig. 7 Tropical Atlantic near-surface winds and zonal wind bias in spring. (a) Same as Fig. 6, but for the zonal component of 10 m wind in WAtl. (b) Climatological mean of observed 10 m wind (arrows) and the Kiel Climate Model (KCM) zonal wind bias in February–April (shading) in the equatorial Atlantic. The wind climatology is based on the Scatterometer Climatology of Ocean Winds (SCOW, Risien and Chelton (2008)). Arrows combine the zonal and meridional components of the climatological 10 m wind, while shading only refers to the zonal component of the wind



dynamics compare to the observed processes that shape the tropical Atlantic climate system? In the next subsection, we first review the basic processes that establish the observed seasonal cycle in the tropical Atlantic, and then compare the observations with what is happening in state-of-the-art climate models.

Which Processes Produce the Equatorial Atlantic Warm Bias?

A good first assumption about the seasonal cycle is that it is driven by the seasonal movement of the sun. Such a seasonal cycle should be symmetric. In the tropical Atlantic, however, it is clearly asymmetric. Figure 6 shows that the cooling period between April and August is much shorter – or, equivalently, more intense – than the subsequent period of gradual warming that lasts until the following April. Processes other

than the seasonal forcing of solar insolation must contribute to the fast growth of the summer cold tongue.

Recent studies of the tropical Atlantic suggest that the rapid formation of the cold tongue involves a coupled, positive feedback (Keenlyside and Latif 2007; Burls et al. 2011; Richter et al. 2016). A feedback establishes a relationship between two or more variables. In a negative feedback small perturbations in one variable are compensated by changes in the other such that the system returns to its original, stable state. The opposite is true for a positive feedback. Here, a perturbation – even a small one – in one variable provokes changes in the other variables that reinforce the original perturbation. The system continues to diverge from its initial state. The perturbation grows until the feedback is disrupted.

The dominant positive feedback in the equatorial oceans is the Bjerknes feedback (Bjerknes 1969). It relates three key properties of an equatorial ocean basin to each other: SST in the eastern ocean basin; zonal wind variability in the western

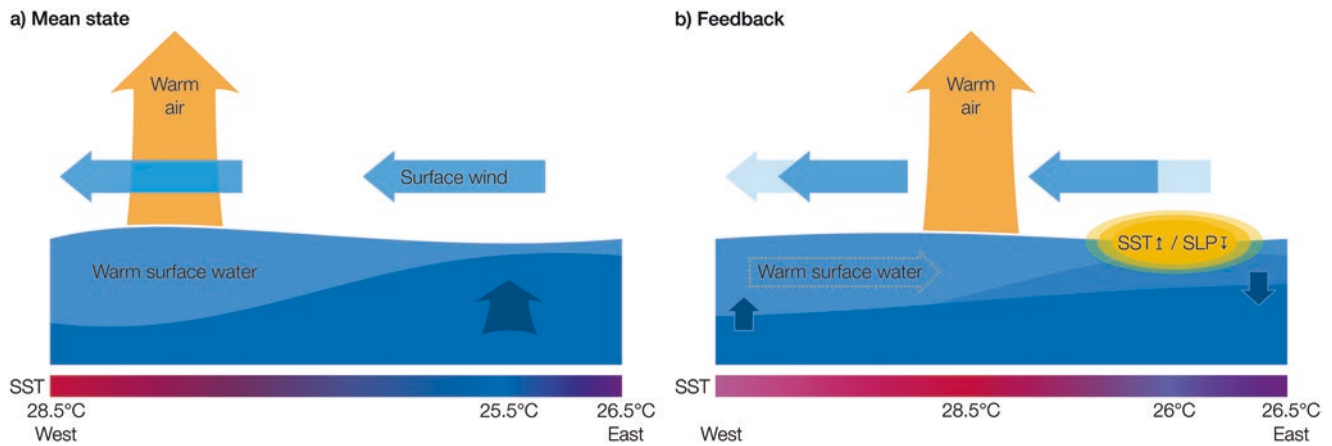


Fig. 8 The Bjerknes feedback. (a) Mean state. Along the equator, the surface wind field is dominated by the trade winds of the southern hemisphere. Both the zonal and meridional components of the trade winds contribute to surface divergences close to the equator, producing equatorial upwelling (thick blue arrow). Steady equatorial easterly wind forcing (blue arrows) pushes warm surface waters (light blue layer) towards the western ocean basin and builds up the warm pool. Warm and moist air rises above the warm pool (orange arrow). In contrast, the surface mixed layer is thin in the eastern basin, upwelling is more efficient there, and SSTs are, on average, cooler than in the warm pool (approximately 25.5 °C and 28.5 °C, respectively; the equatorial SST distribution is sketched in the bar below the figure). (b) The positive Bjerknes feedback alters the state of the tropical ocean. The trade

winds weaken, and zonal surface winds in the western ocean basin decrease. The balance between the subsurface pressure gradient and wind stress forcing is disrupted, and part of the warm pool “sloshes back” into the central ocean basin, redistributing warm surface water more evenly across the ocean basin. The tilt in the interface between the surface and subsurface waters decreases, and upwelling is less efficient in providing cold subsurface water to the surface layer in the eastern ocean basin. The cold tongue region warms (orange ovals). Sea level pressure (SLP) over the warm anomalies decreases, and convection shifts towards the central ocean basin. The surface wind response to this shift in surface convection and the zonal SLP distribution further weakens the trade wind regimes and closes the feedback

ocean basin; and the zonal distribution of upper ocean heat content along the equator, with large heat reservoirs and thick surface layers in the western warm pool, and thin surface layers in the cold tongue region in the east.

Figures 8a and b illustrate, respectively, the mean state of an equatorial ocean and how the Bjerknes feedback alters it. Consider a weakening of the easterly trade winds in the western ocean basin (or equivalently a decrease in easterly zonal wind stress at the ocean surface). The balance between the wind stress and the piled-up warm water in the western ocean basin temporarily fades, and the piled-up warm pool “sloshes back” into the eastern ocean basin, redistributing the upper ocean heat content more evenly across the equatorial basin.⁹ The zonal gradient in heat content is leveled out, and the additional heat in the eastern ocean basin helps to establish a positive SST anomaly. This process can last several months in the equatorial Pacific and approximately

one month in the equatorial Atlantic. (These different time scales are mainly due to the different east-west extents of the basins and hence signal propagation speeds.)

In the tropics, the atmosphere is closely coupled to the ocean. It reacts strongly to underlying SST variability by developing an anomalous wind field that converges over a warmer-than-usual patch of water (Gill 1980). The local changes in the wind field co-occur with changes in the zonal pressure gradient along the equator. The altered zonal pressure gradient in turn induces further weakening of the easterly trade winds in the western ocean basin, closing the feedback loop. An equivalent process with opposite signs takes place when the trade winds intensify in the western ocean basin.

The Bjerknes feedback is restricted to the equatorial ocean basins. While the ingredients of the feedback – wind, upper ocean heat content and SST variability – are present in every region of the ocean and usually interact with each other in one way or the other, the fully coupled Bjerknes feedback requires that information is zonally transmitted across almost the entire zonal extent of the basin, both in the atmosphere and the ocean. This is only possible when the Coriolis force vanishes or is negligibly small, since it would otherwise deflect the involved physical motions into curved movements. A direct, zonal exchange between the eastern and western ocean basins would not be possible in the presence of the Coriolis force.

⁹In the framework of this explanation, an interesting observation is that the Bjerknes feedback can only operate as long as the reservoir of warm water in the western warm pool is not empty. Once this is the case, the feedback breaks down, the SST anomaly stops to grow and the warm pool fills up again. A negative feedback has replaced the positive feedback. For the tropical Pacific, this sequence of alternating feedbacks has been described by Jin (1997) in the framework of the *recharge oscillator*. The name relates to the idea that the equatorial ocean is “charged” with warm water in the warm pool region – or, equivalently, heat – that is then discharged to the atmosphere during a warm event.

In the tropical Atlantic, a number of seasonal processes in the coupled atmosphere-ocean system produce a climate state that allows the Bjerknes feedback to operate during early boreal summer. Although we explain the processes in a sequential manner below, note that clear causalities are hard to establish in a coupled system. Different aspects of the phenomenon – here: the northward movement of the ITCZ and the development of the Atlantic cold tongue – cannot be disentangled from each other. Neither does the ITCZ move north *because* of the cold tongue development, nor does the cold tongue develop *because* the ITCZ moves north. Rather, both phenomena co-occur as manifestations of the same coupled phenomenon.

One key ingredient of the equatorial Atlantic seasonal cycle is the northward migration of the marine ITCZ (Xie and Philander 1994). In boreal spring, the ITCZ is in its southernmost position. The trade wind regimes of both hemispheres converge close to the equator and produce weak equatorial surface winds. When the ITCZ moves north in late boreal spring, the southern hemisphere trade winds cross the equator. Starting in March–April, surface winds intensify (illustrated by an increase in magnitude in Fig. 7a) and contribute to enhanced equatorial upwelling.

The spring strengthening of western equatorial zonal surface winds enhances the zonal gradient in upper ocean heat content. Strong easterly winds push the surface waters more efficiently towards the western warm pool, thinning out the warm surface layer in the eastern ocean basin and transporting the cooling signal westward. As a result, cold subsurface water lodges closer to the ocean surface. This background state requires very little subsurface water to be mixed into the surface layer to produce a substantial cooling. The western equatorial zonal spring winds “precondition” the eastern equatorial Atlantic for the formation of the cold tongue (e.g., Merle 1980; Okumura and Xie 2006; Grodsky et al. 2008; Hormann and Brandt 2009; Marin et al. 2009).

In concert with the development of the first seasonal cooling signals in May and June, the West African monsoon sets in (e.g., Okumura and Xie 2004; Brandt et al. 2011b; Caniaux et al. 2011; Giannini et al. 2003). From an atmospheric perspective, the monsoon onset is characterized by accelerating southeasterly surface winds in the Gulf of Guinea in late boreal spring. The strengthening *meridional* component of these winds enhances upwelling slightly to the south of the equator, and downwelling slightly to the north. The intensified upwelling provides additional initial cooling to the eastern equatorial region by mixing colder subsurface water into the warm surface layer. From the ocean perspective, on the other hand, cooling SSTs in the eastern equatorial Atlantic intensify the southerly winds in the Gulf of Guinea, which in turn contributes to the northward migration of convection and rainfall associated with the West African monsoon (Okumura and Xie 2004).

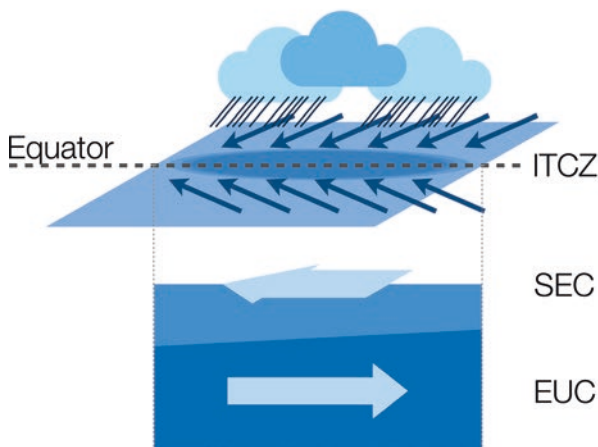
Lastly, oceanic processes contribute to the formation of the cold tongue. A number of studies found that vertical mixing at the base of the surface layer – where temperature gradients are strongest – seasonally varies in strength (e.g., Hazeleger and Haarsma 2005; Jouanno et al. 2011; Hummels et al. 2013, 2014). A likely explanation for this is that the intensities of the westward surface current and the eastward equatorial undercurrent vary over the course of the year. When the relative velocities of the two currents are strong, the vertical velocity shear at their boundary increases,¹⁰ and frictional processes mix colder subsurface water into the warm surface layer. Figure 9 illustrates both the spring state of the tropical Atlantic and the basic processes that produce the first cooling signals in early boreal summer.

The net effect of these interacting processes – the northward migration of the ITCZ and the associated strengthening of the southern hemisphere trade winds on the equator, the thinning of the eastern equatorial surface layer, the enhanced upwelling along the equator and especially in the cold tongue region, and the increased mixing at the base of the surface mixed layer – is that the first cold anomalies develop in the eastern equatorial Atlantic in late April. The atmosphere in turn reacts to the cold anomalies, and the Bjerknes feedback sets in. Starting in May, it lends additional growth to the cold tongue (Burls et al. 2011). In August, the seasonally active Bjerknes feedback loop breaks down (Dippe et al. 2017) and a more moderate warming sets in. In the absence of the Bjerknes feedback the cold tongue can no longer be maintained and dissolves, due to mixing processes in the ocean and surface heat exchange with the atmosphere.

Many models struggle to simulate a seasonally active Bjerknes feedback that is comparable to observations in both strength and seasonality. Richter and Xie (2008) pointed out that model performance with respect to the Atlantic Bjerknes feedback is quite diverse between models that participated in the Coupled Model Intercomparison Project, Phase 3 (CMIP3, Meehl et al. 2007). Likewise, Deppenmeier et al. (2016) found systematic weaknesses in the CMIP5 models. For example, many models displace the Atlantic warm pool towards the central equatorial Atlantic (Chang et al. 2007; Richter and Xie 2008; Liu et al. 2013). This displacement is a consequence of the westerly wind bias in the western equatorial Atlantic (Wahl et al. 2011; Richter et al. 2012, 2014b). Figure 7 illustrates for the KCM that the spring winds are much weaker in the model than in observations. Consequently, the surface wind stress is not sufficient to pile up warm sur-

¹⁰“Velocity shear” is a different term for “velocity gradient”. A flow is sheared when different layers of the flow have different velocities. Depending on the magnitude of the shear and the viscosity of the fluid, the shear produces local turbulence and mixing due to frictional processes within the fluid. If no turbulence occurs, the flow is called “laminar”.

a) Boreal spring



b) Initial cooling

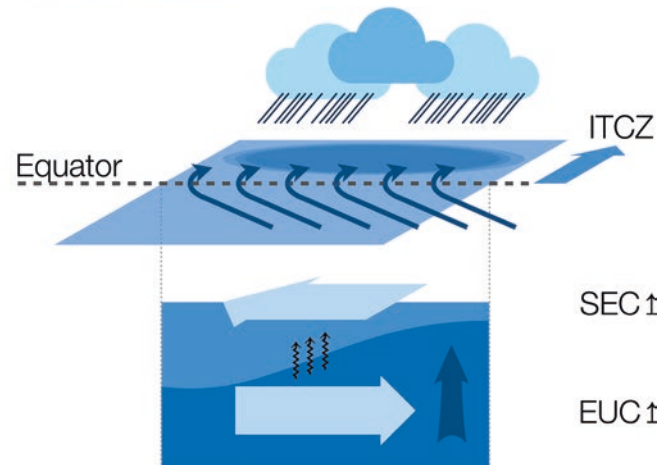


Fig. 9 Initial cold tongue cooling in the tropical Atlantic. **(a)** Spring conditions. The highest sea surface temperatures (SSTs) and the lowest sea level pressures (SLPs) are found approximately on the equator (dashed black line), forming the equatorial low pressure trough (dark-blue shading). The trade wind systems of both the northern and the southern hemispheres (dark blue arrows) converge in the trough and anchor the Inter-Tropical Convergence Zone (ITCZ, clouds and strong precipitation) to the equator. Zonal surface wind forcing is relaxed during spring, warm surface waters are distributed more evenly across the basin. At the ocean surface, the South Equatorial Current (SEC) transports water towards the west. Below the surface, close to the interface between the surface layer and the subsurface, the Equatorial Undercurrent (EUC) transports water towards the east. **(b)** Initial cold tongue cooling: In early boreal summer, the ITCZ migrates away from the

equator into the northern hemisphere. The trade winds of the southern hemisphere follow the low pressure trough and cross the equator. In the western ocean basin, zonal surface winds increase and push the warm surface water more efficiently towards the west. The warm pool deepens in the west, while the surface layer thins in the east. Additionally, both the meridional and zonal components of the wind field in the eastern ocean basin strengthen and contribute to a local surface divergence that is compensated by enhanced upwelling (thick, dark-blue arrow). Lastly, both the SEC and EUC increase in strength. Enhanced vertical velocity gradients in the vicinity of the interface between the surface and the subsurface water layers produce shear instabilities (black squiggly lines) that mix the cold subsurface water efficiently into the surface layer

face waters in the western ocean basin in a manner comparable to observations. Heat content is distributed more evenly across the equatorial ocean basin and supplies additional heat to the eastern surface layer. Even if the model produced wind variability that could serve as a valid initial perturbation to trigger the Bjerknes feedback,¹¹ the biased background state of the ocean could not support the feedback. The cold tongue fails to establish.

An interesting equivalent of this mechanism has been observed in the real ocean by Marin et al. (2009). The study compares the Atlantic cold tongue in two years with grossly different wind variability and finds that in the year with relatively weak spring winds in the western equatorial Atlantic – this compares well to the climatological, biased state in many CGCMs –, the zonal heat content gradient in the upper ocean does not develop. The winds fail to precondition the tropical Atlantic for the growth of the cold tongue.

Studies with current atmospheric GCMs have found the westerly wind bias in boreal spring to be an intrinsic feature of (uncoupled) atmospheric GCMs (Richter et al. 2012,

2014b; Harlaß et al. 2017). Coupling an already biased atmospheric GCM to an ocean GCM induces positive feedbacks that amplify the wind and SST biases in the equatorial Atlantic. Additionally, Grodsky et al. (2012) showed that an ocean GCM, too, is intrinsically biased in the tropical Atlantic, although the magnitude of this bias is much smaller than the warm bias in a coupled model.

The atmospheric westerly wind bias has been linked to a seesaw pattern in rainfall biases over South America and Africa (Chang et al. 2007; Richter et al. 2012, 2014b; Patricola et al. 2012). The proposed physical mechanism that links precipitation to the wind is the following: Tropical rainfall is tied to strong convection. Ascending moist and warm air masses create a local negative pressure anomaly at the surface that alters the zonal gradient in surface pressure along the equator. Surface winds, in turn, are dynamically related to surface pressure gradients.¹²

A current hypothesis of what prevents climate models from developing a cold tongue comparable to observations in

¹¹This is by no means a given. As shown below and hinted at above, the equatorial Atlantic bias also manifests in the atmosphere and may well prevent the model from establishing the link between eastern ocean SST and western ocean wind variability that is necessary to close the Bjerknes feedback loop.

¹²Wind compensates pressure gradients. That is why large-scale storm systems are organized around low core pressures: The storm winds try to flow into the low pressure at the “heart” of the storm and eliminate the strong pressure gradient between the storm center and the storm environment. The Coriolis force provides rotation to storm systems by deflecting the pressure compensation flow.

boreal summer thus is: Opposing rainfall biases in South America and Africa produce a zonal surface pressure gradient along the equator that is weaker than in observations. The resulting winds in the equatorial western Atlantic are too weak in magnitude and cannot reproduce the observed distribution of upper ocean heat content. Consequently, the seasonally induced equatorial upwelling in early boreal summer is not sufficient to produce the observed cooling that finally triggers the Bjerknes feedback.

In agreement with these mechanisms, a number of studies have found that a physically sound way to reduce the equatorial Atlantic warm bias is to improve the atmospheric models. Tozuka et al. (2011) showed that tweaking the convection scheme can project strongly on the ability of the models to simulate the correct distribution of climatological SSTs in the equatorial Atlantic. Harlaß et al. (2015) conducted a number of experiments with the KCM that varied both the horizontal and vertical resolution of the atmospheric GCM, while keeping a constant coarse resolution for the ocean GCM. For sufficiently high atmospheric resolutions, the western equatorial wind bias strongly decreased and the equatorial Atlantic warm bias nearly vanished. The seasonal cycle as a whole greatly improved. In a follow-up study, Harlaß et al. (2017) found that sea level pressure and precipitation gradients along the equator are not sensitive to the atmospheric resolution. Nevertheless, the wind bias in their study decreased significantly. To explain this, they propose that the position of maximum precipitation and zonal momentum transport play an important role in giving rise to the zonal wind bias. Zonal momentum can be either transported by mixing it from the free troposphere into the boundary layer or by meridional advection into the western equatorial Atlantic (Zermeño-Díaz and Zhang 2013; Richter et al. 2014b, 2017). These findings agree with the study of Richter et al. (2014a), who found that zonal wind variability in the western equatorial Atlantic is strongly related to vertical momentum transports in the overlying atmosphere. Further studies by Voltaire et al. (2014), Wahl et al. (2011), and DeWitt (2005) confirm the importance of the atmospheric component of a CGCM to properly simulate the complex tropical Atlantic climate system.

Outlook: Implications for the Usability of CGCMs in the Equatorial Atlantic

Using the KCM, a CGCM that simulates the tropical Atlantic in a manner very similar to a wide range of state-of-the-art CGCMs, we have shown exemplarily that coupled global climate models currently struggle to simulate a realistic equatorial Atlantic climate system. The dominant feature of this problem is that CGCMs struggle to simulate the defining feature of the seasonal cycle – the formation of the Atlantic

cold tongue in early boreal summer. An important cause of this bias is a strong and seasonally varying westerly wind bias in equatorial zonal wind in atmospheric models that is present even in the absence of atmosphere-ocean coupling. While much progress has been made in understanding and reducing the equatorial Atlantic warm bias, many models still produce a profoundly unrealistic seasonal cycle in the equatorial Atlantic. How does this shortcoming affect the usefulness of coupled models in the equatorial Atlantic?

A key task of climate models is to forecast deviations from the expected climate state. For seasonal predictions, the expected climate state is the climatological seasonal cycle. Some of these deviations are generated randomly and are, by definition, unpredictable. Others are the product of – sometimes potentially predictable – climate variability.

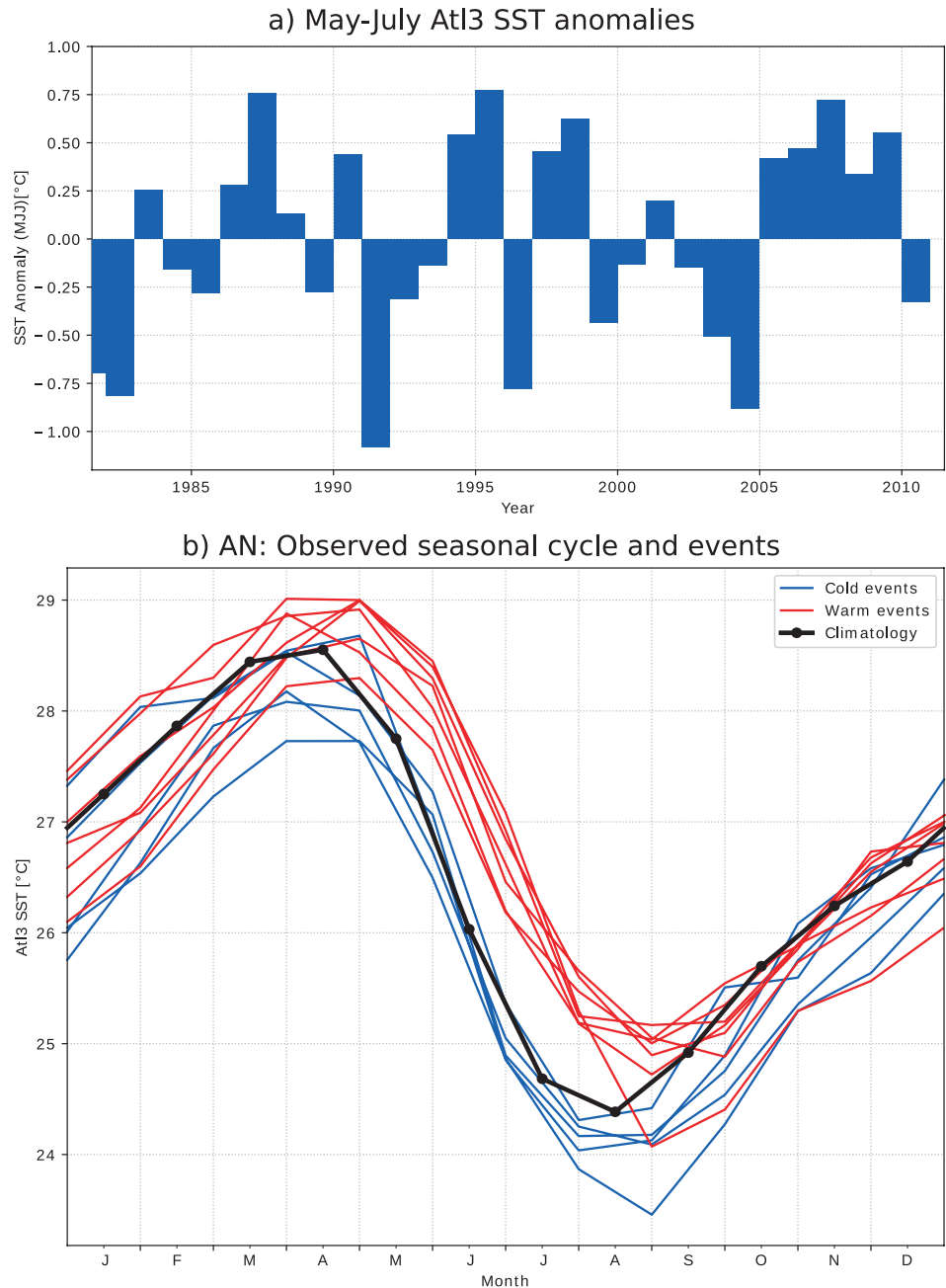
In the tropical Atlantic, the dominant mode of year-to-year SST variability is the Atlantic Niño¹³ (Zebiak 1993). The Atlantic Niño is essentially a modulation of the seasonal formation of the cold tongue (Burls et al. 2012). This modulation can manifest in a range of different cold tongue measures. For example, cold tongue growth might set in earlier (or later), the cold tongue might cool more strongly, or it might, in its mature phase, occupy a larger area in the tropical Atlantic than usual. Caniaux et al. (2011) argued that all of these measures reveal an aspect of cold tongue variability, but that they do not vary consistently with each other.

Still, the Atlantic Niño is generally described in terms of Atl3 summer SSTs. While the seasonal cycle of Atl3 SSTs spans a range of roughly 5 °C, interannual variations of Atl3 SST between May and July rarely exceed amplitudes of 1 °C (Fig. 10a). The seasonal cycle of the tropical Atlantic is by far the dominant signal in Atl3 SSTs (Fig. 10b). It is the background against which the interannual variability of the Atlantic Niño plays out.

Even though the Atlantic Niño constitutes only a relatively small deviation from the seasonal cycle, its effects on adjacent rainfall patterns can be substantial (e.g., Giannini et al. 2003; García-Serrano et al. 2008; Polo et al. 2008; Rodríguez-Fonseca et al. 2011). A key demand of African countries, where food security heavily relies on agriculture, is hence to be able to reliably predict the amplitude of the Atlantic Niño a few months, ideally even more than a season, ahead. Only such relatively long-ranged forecasts would allow African farmers to adapt their farming strategy

¹³The name “Atlantic Niño” refers to the Pacific El Niño, because the pattern of Atlantic Niño SST anomalies is similar to the Pacific El Niño. Apart from this, a number of differences exist between the two phenomena (discussed for example in Keenlyside and Latif (2007), Burls et al. (2011), Lübbecke and McPhaden (2012), Richter et al. (2013), and Lübbecke and McPhaden (2017)). Nnamchi et al. (2015, 2016) argued that the Atlantic Niño might not be dynamical in nature, but a product of atmospheric noise forcing. Alternative names for the Atlantic Niño are Atlantic Zonal Mode or Atlantic Cold Tongue Mode.

Fig. 10 The observed Atlantic Niño, based on the NOAA Optimum Interpolated SST dataset (OISST). (a) Time series of May–June–July (MJJ) Atl3 sea surface temperature (SST) anomalies. (Anomalies of a time series that, for each year, averaged MJJ monthly means together. Positive values indicate that the observed Atl3 region was warmer in MJJ of that year than on average.) (b) Observed seasonal cycle of Atl3 SST (black) and SST trajectories for individual years that produced warm (red) and cold (blue) Atlantic Niño events



for the upcoming season. Unfortunately, most models perform very poorly with respect to the Atlantic Niño and can provide hardly any predictive skill (Stockdale et al. 2006; Richter et al. 2017).

One reason for these shortcomings is that a prerequisite to simulate the variability of Atlantic cold tongue growth is a model that produces a realistic cold tongue. Indeed, Ding et al. (2015) showed that even a symptomatic – as opposed to a dynamically motivated and hence more process-oriented – reduction of the equatorial Atlantic SST bias in the KCM greatly improves the ability of the model to track the observed Atlantic Niño variability. This serves as an example of how the mean state interacts with climate variability. How the

bias influences the predictive skill of the KCM for tropical Atlantic SST and whether the real climate system actually provides the potential to produce reliable forecasts of Atlantic Niño variability a few months in advance are the subjects of current research.

In general, the equatorial Atlantic warm bias has been an important issue since the earliest attempts of coupled global climate modeling (Davey et al. 2002) and continues to challenge the scientific community. It serves as an important reminder that model output should not always be taken at face value. Rather, models can struggle to represent observed physical processes, even though their physical basis in the form of the approximated Navier-Stokes equations is sound.

In the equatorial Atlantic, the entire coupled system is off-key in coupled global climate models due to the misrepresentation of crucial physical processes. However, alternative ways exist to study the tropical Atlantic with the help of models. Akin to early modeling studies of the El Niño–Southern Oscillation, statistical models can provide some insight into the equatorial Atlantic (e.g., Wang and Chang 2008; Chang et al. 2004). Simulations with ocean-only GCMs help to understand the oceanic response to atmospheric processes (e.g., Lübbecke et al. 2010). Additionally, regional climate models of the equatorial Atlantic have been employed successfully to study different aspects of the region (e.g., Seo et al. 2006; Burls et al. 2011, 2012). Lastly, computational power continues to increase and allows for higher spatial resolution. If the equatorial Atlantic contains predictive potential, future generations of improved CGCMs are likely to unlock it at some point.

The research into various biases, their origins, their dynamics, and, most importantly, possible ways to reduce them, remains a core challenge of the global climate modeling community.

Acknowledgements We would like to thank Richard Greatbatch, Peter Brandt, Mojib Latif, Rebecca Hummels, and Martin Claus for discussing the manuscript with us at an early stage and contributing valuable ideas.

While we finished work on the first submitted draft of the manuscript, our colleague and friend Martin Krebs passed away. We hope this study will serve as a reminder of Martin’s outstanding scientific work. TD will fondly remember how she discussed first ideas for the manuscript with Martin and how they came up with a rather wayward way to illustrate how much energy was lost from the Atl3 region during the formation of the cold tongue. Turns out that 2.6 times the total global energy consumption of 2011 is enough to power roughly 70 billion generic 600 W fridges for 4 months.

Appendix

This article is related to the YOUNARES 8 conference session no. 3: “Physical Processes in the Tropical and Subtropical Oceans: Variability, Impacts, and Connections to Other Components of the Climate System”. The original Call for Abstracts and the abstracts of the presentations within this session can be found in the appendix “Conference Sessions and Abstracts”, chapter “1 Physical Processes in the Tropical and Subtropical Oceans: Variability, Impacts, and Connections to Other Components of the Climate System”, of this book.

References

- Banzon V, Smith TM, Chin TM et al (2016) A long-term record of blended satellite and in situ sea-surface temperature for climate monitoring, modeling and environmental studies. *Earth Syst Sci Data* 8(1):165–176. <https://doi.org/10.5194/essd-8-165-2016>
- Bjerknes J (1969) Atmospheric teleconnections from the equatorial Pacific. *Mon Weather Rev* 97(3):163–172
- Bourlès B, Lumpkin R, McPhaden MJ et al (2008) The Pirata program: history, accomplishments, and future directions. *Bull Am Meteorol Soc* 89(8):1111–1125. <https://doi.org/10.1175/2008BAMS2462.1>
- Brandt P, Schott FA, Provost C et al (2006) Circulation in the central equatorial Atlantic: mean and intraseasonal to seasonal variability. *Geophys Res Lett* 33(7):L07609. <https://doi.org/10.1029/2005GL025498>
- Brandt P, Hormann V, Bourlès B et al (2008) Oxygen tongues and zonal currents in the equatorial Atlantic. *J Geophys Res Oceans* 113(4):C04012. <https://doi.org/10.1029/2007JC004435>
- Brandt P, Caniaux G, Bourlès B et al (2011a) Equatorial upper-ocean dynamics and their interaction with the West African monsoon. *Atmos Sci Lett* 12(1):24–30. <https://doi.org/10.1002/asl.287>
- Brandt P, Funk A, Hormann V et al (2011b) Interannual atmospheric variability forced by the deep equatorial Atlantic ocean. *Nature* 473(7348):497–500. <https://doi.org/10.1038/nature10013>
- Burls NJ, Reason CJC, Penven P et al (2011) Similarities between the tropical Atlantic seasonal cycle and ENSO: an energetics perspective. *J Geophys Res Oceans* 116(C11):C11010. <https://doi.org/10.1029/2011JC007164>
- Burls NJ, Reason CJC, Penven P et al (2012) Energetics of the tropical Atlantic zonal mode. *J Clim* 25(21):7442–7466. <https://doi.org/10.1175/JCLI-D-11-00602.1>
- Caniaux G, Giordani H, Redelsperger JL et al (2011) Coupling between the Atlantic cold tongue and the West African monsoon in boreal spring and summer. *J Geophys Res Oceans* 116(4):C04003. <https://doi.org/10.1029/2010JC006570>
- Chang P, Saravanan R, Wang F et al (2004) Predictability of linear coupled systems. Part II: an application to a simple model of tropical Atlantic variability. *J Clim* 17(7):1487–1503. [https://doi.org/10.1175/1520-0442\(2004\)017<1487:POLCSP>2.0.CO;2](https://doi.org/10.1175/1520-0442(2004)017<1487:POLCSP>2.0.CO;2)
- Chang CY, Carton JA, Grodsky SA et al (2007) Seasonal climate of the tropical Atlantic sector in the NCAR community climate system model 3: error structure and probable causes of errors. *J Clim* 20(6):1053–1070. <https://doi.org/10.1175/JCLI4047.1>
- Cromwell T (1953) Circulation in a meridional plane in the central equatorial Pacific. *J Mar Res* 23:196–213
- Cromwell T, Montgomery RB, Stroup ED (1954) Equatorial undercurrent in Pacific ocean revealed by new methods. *Science* 119(3097):648–649. <https://doi.org/10.1126/science.119.3097.648>
- Davey M, Huddleston M, Sperber K et al (2002) STOIC: a study of coupled model climatology and variability in tropical ocean regions. *Clim Dyn* 18(5):403–420. <https://doi.org/10.1007/s00382-001-0188-6>
- Deppenmeier AL, Haarsma RJ, Hazeleger W (2016) The Bjerknes feedback in the tropical Atlantic in CMIP5 models. *Clim Dyn* 47(7–8):2691–2707. <https://doi.org/10.1007/s00382-016-2992-z>
- DeWitt DG (2005) Diagnosis of the tropical Atlantic near-equatorial SST bias in a directly coupled atmosphere-ocean general circulation model. *Geophys Res Lett* 32(1):L01703. <https://doi.org/10.1029/2004GL021707>
- Ding H, Greatbatch RJ, Latif M et al (2015) The impact of sea surface temperature bias on equatorial Atlantic interannual variability in partially coupled model experiments. *Geophys Res Lett* 42(13):5540–5546. <https://doi.org/10.1002/2015GL064799>
- Dippe T, Greatbatch RJ, Ding H (2017) On the relationship between Atlantic Niño variability and ocean dynamics. *Clim Dyn*. <https://doi.org/10.1007/s00382-017-3943-z>
- Doi T, Vecchi GA, Rosati AJ et al (2012) Biases in the Atlantic ITCZ in seasonal-interannual variations for a coarse- and a high-resolution coupled climate model. *J Clim* 25(16):5494–5511. <https://doi.org/10.1175/JCLI-D-11-00360.1>
- Foltz GR, McPhaden MJ (2010) Interaction between the Atlantic meridional and Niño modes. *Geophys Res Lett* 37:L18604. <https://doi.org/10.1029/2010GL044001>

- Fretwell P, Pritchard HD, Vaughan DG et al (2013) Bedmap2: improved ice bed, surface and thickness datasets for Antarctica. *Cryosphere* 7(1):375–393. <https://doi.org/10.5194/tc-7-375-2013>
- Frierson DMW, Hwang YT, Fučkar NS et al (2013) Contribution of ocean overturning circulation to tropical rainfall peak in the northern hemisphere. *Nat Geosci* 6:940–944. <https://doi.org/10.1038/ngeo1987>
- García-Serrano J, Losada T, Rodríguez-Fonseca B et al (2008) Tropical Atlantic variability modes (1979–2002). Part II: time-evolving atmospheric circulation related to SST-forced tropical convection. *J Clim* 21(24):6476–6497. <https://doi.org/10.1175/2008JCLI2191.1>
- Giannini A, Saravanan R, Chang P (2003) Oceanic forcing of Sahel rainfall on interannual to interdecadal time scales. *Science* 302(5647):1027–1030. <https://doi.org/10.1126/science.1089357>
- Gill AE (1980) Some simple solutions for heat-induced tropical circulation. *Q J R Meteorol Soc* 106(449):447–462. <https://doi.org/10.1002/qj.49710644905>
- Grodsky SA, Carton JA, McClain CR (2008) Variability of upwelling and chlorophyll in the equatorial Atlantic. *Geophys Res Lett* 35(3):L03610. <https://doi.org/10.1029/2007GL032466>
- Grodsky SA, Carton JA, Nigam S et al (2012) Tropical Atlantic biases in CCSM4. *J Clim* 25(11):3684–3701. <https://doi.org/10.1175/JCLI-D-11-00315.1>
- Harlaß J, Latif M, Park W (2015) Improving climate model simulation of tropical Atlantic sea surface temperature: the importance of enhanced vertical atmosphere model resolution. *Geophys Res Lett* 42(7):2401–2408. <https://doi.org/10.1002/2015GL063310>
- Harlaß J, Latif M, Park W (2017) Alleviating tropical Atlantic sector biases in the Kiel climate model by enhancing horizontal and vertical atmosphere model resolution: climatology and interannual variability. *Clim Dyn* 50:2605. <https://doi.org/10.1007/s00382-017-3760-4>
- Hastenrath S (1991) *Climate dynamics of the tropics*. Springer, Dordrecht. <https://doi.org/10.1007/978-94-011-3156-8>
- Hazeleger W, Haarsma RJ (2005) Sensitivity of tropical Atlantic climate to mixing in a coupled ocean-atmosphere model. *Clim Dyn* 25(4):387–399. <https://doi.org/10.1007/s00382-005-0047-y>
- Hormann V, Brandt P (2009) Upper equatorial Atlantic variability during 2002 and 2005 associated with equatorial Kelvin waves. *J Geophys Res Oceans* 114:C03007. <https://doi.org/10.1029/2008JC005101>
- Hummels R, Dengler M, Bourlès B (2013) Seasonal and regional variability of upper ocean diapycnal heat flux in the Atlantic cold tongue. *Prog Oceanogr* 111:52–74. <https://doi.org/10.1016/j.pocean.2012.11.001>
- Hummels R, Dengler M, Brandt P et al (2014) Diapycnal heat flux and mixed layer heat budget within the Atlantic cold tongue. *Clim Dyn* 43(11):3179–3199. <https://doi.org/10.1007/s00382-014-2339-6>
- Jin FF (1997) An equatorial ocean recharge paradigm for ENSO. Part I: conceptual model. *J Atmos Sci* 54(7):811–829
- Johns WE, Brandt P, Bourlès B et al (2014) Zonal structure and seasonal variability of the Atlantic equatorial undercurrent. *Clim Dyn* 43(11):3047–3069. <https://doi.org/10.1007/s00382-014-2136-2>
- Jouanno J, Marin F, Du Penhoat Y et al (2011) Seasonal heat balance in the upper 100 m of the equatorial Atlantic Ocean. *J Geophys Res Oceans* 116(9):C09003. <https://doi.org/10.1029/2010JC006912>
- Keenlyside NS, Latif M (2007) Understanding equatorial Atlantic interannual variability. *J Clim* 20(1):131–142. <https://doi.org/10.1175/JCLI3992.1>
- Liu H, Wang C, Lee SK et al (2013) Atlantic warm pool variability in the CMIP5 simulations. *J Clim* 26(15):5315–5336. <https://doi.org/10.1175/JCLI-D-12-00556.1>
- Locarnini RA, Mishonov AV, Antonov JJ et al (2013) *World ocean atlas 2013*. Vol. 1: Temperature. Levitus S (ed), Mishonov A (technical ed), NOAA Atlas NESDIS 73
- Lübbecke JF, McPhaden MJ (2012) On the inconsistent relationship between Pacific and Atlantic Niños. *J Clim* 25(12):4294–4303. <https://doi.org/10.1175/JCLI-D-11-00553.1>
- Lübbecke JF, McPhaden MJ (2017) Symmetry of the Atlantic Niño mode. *Geophys Res Lett* 44(2):965–973. <https://doi.org/10.1002/2016GL071829>
- Lübbecke JF, Böning CW, Keenlyside NS et al (2010) On the connection between Benguela and equatorial Atlantic Niños and the role of the South Atlantic anticyclone. *J Geophys Res Oceans* 115(C9):C09015. <https://doi.org/10.1029/2009JC005964>
- Lübbecke JF, Burls NJ, Reason CJC et al (2014) Variability in the South Atlantic anticyclone and the Atlantic Niño mode. *J Clim* 27(21):8135–8150. <https://doi.org/10.1175/JCLI-D-14-00202.1>
- Madec G (2008) *NEMO ocean general circulation model reference manual*. Tech. rep., Institut Pierre-Simon Laplace, Paris
- Marin F, Caniaux G, Giordani H et al (2009) Why were sea surface temperatures so different in the eastern equatorial Atlantic in June 2005 and 2006? *J Phys Oceanogr* 39(6):1416–1431. <https://doi.org/10.1175/2008JPO4030.1>
- McPhaden MJ (1995) The tropical atmosphere ocean array is completed. *Bull Am Meteorol Soc* 76:739–741
- McPhaden MJ, Meyers G, Ando K et al (2009) RAMA: the research moored Array for African-Asian-Australian monsoon analysis and prediction. *Bull Am Meteorol Soc* 90(4):459–480. <https://doi.org/10.1175/2008BAMS2608.1>
- Meehl GA, Covey C, Taylor KE et al (2007) THE WCRP CMIP3 multimodel dataset: a new era in climate change research. *Bull Am Meteorol Soc* 88(9):1383–1394. <https://doi.org/10.1175/BAMS-88-9-1383>
- Merle J (1980) Seasonal heat budget in the equatorial Atlantic ocean. *J Phys Oceanogr* 10(3):464–469
- Mitchell TP, Wallace JM (1992) The annual cycle in equatorial convection and sea surface temperature. *J Clim* 5(10):1140–1156
- Nnamchi HC, Li J, Kucharski F et al (2015) Thermodynamic controls of the Atlantic Niño. *Nat Commun* 6:8895. <https://doi.org/10.1038/ncomms9895>
- Nnamchi HC, Li J, Kucharski F et al (2016) An equatorial-extratropical dipole structure of the Atlantic Niño. *J Clim* 29(20):7295–7311. <https://doi.org/10.1175/JCLI-D-15-0894.1>
- Okumura Y, Xie SP (2004) Interaction of the Atlantic equatorial cold tongue and the African monsoon. *J Clim* 17(18):3589–3602. [https://doi.org/10.1175/1520-0442\(2004\)017<3589:IOTAEC>2.0.CO;2](https://doi.org/10.1175/1520-0442(2004)017<3589:IOTAEC>2.0.CO;2)
- Okumura Y, Xie SP (2006) Some overlooked features of tropical Atlantic climate leading to a new Niño-like phenomenon. *J Clim* 19(22):5859–5874
- Park W, Keenlyside N, Latif M et al (2009) Tropical Pacific climate and its response to global warming in the Kiel climate model. *J Clim* 22(1):71–92. <https://doi.org/10.1175/2008JCLI2261.1>
- Patricola CM, Li M, Xu Z et al (2012) An investigation of tropical Atlantic bias in a high-resolution coupled regional climate model. *Clim Dyn* 39(9):2443–2463. <https://doi.org/10.1007/s00382-012-1320-5>
- Philander SGH, Pacanowski RC (1981) The oceanic response to cross-equatorial winds (with application to coastal upwelling in low latitudes). *Tellus* 33(2):201–210. <https://doi.org/10.3402/tellusa.v33i2.10708>
- Phillips NA (1956) The general circulation of the atmosphere: a numerical experiment. *Q J R Meteorol Soc* 82(352):123–164. <https://doi.org/10.1002/qj.49708235202>
- Polo I, Rodríguez-Fonseca B, Losada T et al (2008) Tropical Atlantic variability modes (1979–2002). Part I: time-evolving SST modes related to West African rainfall. *J Clim* 21(24):6457–6475. <https://doi.org/10.1175/2008JCLI2607.1>
- Reynolds RW, Smith TM, Liu C et al (2007) Daily high-resolution-blended analyses for sea surface temperature. *J Clim* 20(22):5473–5496. <https://doi.org/10.1175/2007JCLI1824.1>
- Rhein M, Dengler M, Sültenfuß J et al (2010) Upwelling and associated heat flux in the equatorial Atlantic inferred from helium isotope disequilibrium. *J Geophys Res Oceans* 115(C8):C08021. <https://doi.org/10.1029/2009JC005772>

- Richter I, Xie SP (2008) On the origin of equatorial Atlantic biases in coupled general circulation models. *Clim Dyn* 31(5):587–598. <https://doi.org/10.1007/s00382-008-0364-z>
- Richter I, Xie SP, Wittenberg AT et al (2012) Tropical Atlantic biases and their relation to surface wind stress and terrestrial precipitation. *Clim Dyn* 38(5–6):985–1001. <https://doi.org/10.1007/s00382-011-1038-9>
- Richter I, Behera SK, Masumoto Y et al (2013) Multiple causes of interannual sea surface temperature variability in the equatorial Atlantic Ocean. *Nat Geosci* 6(1):43–47. <https://doi.org/10.1038/ngeo1660>
- Richter I, Behera SK, Doi T et al (2014a) What controls equatorial Atlantic winds in boreal spring? *Clim Dyn* 43(11):3091–3104. <https://doi.org/10.1007/s00382-014-2170-0>
- Richter I, Xie SP, Behera SK et al (2014b) Equatorial Atlantic variability and its relation to mean state biases in CMIP5. *Clim Dyn* 42(1–2):171–188. <https://doi.org/10.1007/s00382-012-1624-5>
- Richter I, Xie SP, Morioka Y et al (2016) Phase locking of equatorial Atlantic variability through the seasonal migration of the ITCZ. *Clim Dyn* 48(11–12):3615–3629. <https://doi.org/10.1007/s00382-016-3289-y>
- Richter I, Doi T, Behera SK et al (2017) On the link between mean state biases and prediction skill in the tropics: an atmospheric perspective. *Clim Dyn* 50:3355. <https://doi.org/10.1007/s00382-017-3809-4>
- Risien CM, Chelton DB (2008) A global climatology of surface wind and wind stress fields from eight years of QuikSCAT scatterometer data. *J Phys Oceanogr* 38(11):2379–2413. <https://doi.org/10.1175/2008JPO3881.1>
- Rodríguez-Fonseca B, Janicot S, Mohino E et al (2011) Interannual and decadal SST-forced responses of the West African monsoon. *Atmos Sci Lett* 12(1):67–74. <https://doi.org/10.1002/asl.308>
- Roeckner E, Bäuml G, Bonaventura L et al (2003) The atmospheric general circulation model ECHAM5: part 1: model description. *MPI Report* 349. <https://doi.org/10.1029/2010JD014036>
- Roemmich D, Johnson GC, Riser S et al (2009) The Argo program. *Oceanography* 22(2):34–43. <https://doi.org/10.5670/oceanog.2009.36>
- Schott FA, Dengler M, Brandt P et al (2003) The zonal currents and transports at 35°W in the tropical Atlantic. *Geophys Res Lett* 30(7):1349. <https://doi.org/10.1029/2002GL016849>
- Sein DV, Danilov S, Biastoch A et al (2016) Designing variable ocean model resolution based on the observed ocean variability. *J Adv Model Earth Syst* 8(2):904–916. <https://doi.org/10.1002/2016MS000650>
- Seo H, Jochum M, Murtugudde R et al (2006) Effect of ocean mesoscale variability on the mean state of tropical Atlantic climate. *Geophys Res Lett* 33(9):L09606. <https://doi.org/10.1029/2005GL025651>
- Siongco AC, Hohenegger C, Stevens B (2015) The Atlantic ITCZ bias in CMIP5 models. *Clim Dyn* 45(5):1169–1180. <https://doi.org/10.1007/s00382-014-2366-3>
- Stockdale TN, Balmaseda MA, Vidard A (2006) Tropical Atlantic SST prediction with coupled ocean-atmosphere GCMs. *J Clim* 19(23):6047–6061. <https://doi.org/10.1175/JCLI3947.1>
- Sutton RT, Jewson SP, Rowell DP (2000) The elements of climate variability in the tropical Atlantic region. *J Clim* 13(18):3261–3284
- Taylor KE, Stouffer RJ, Meehl GA (2012) An overview of CMIP5 and the experiment design. *Bull Am Meteorol Soc* 93(4):485–498. <https://doi.org/10.1175/BAMS-D-11-00094.1>
- Tozuka T, Doi T, Miyasaka T et al (2011) Key factors in simulating the equatorial Atlantic zonal sea surface temperature gradient in a coupled general circulation model. *J Geophys Res Oceans* 116(6):C06010. <https://doi.org/10.1029/2010JC006717>
- Trenberth KE, Caron JM (2001) Estimates of meridional atmosphere and ocean heat transports. *J Clim* 14(16):3433–3443
- Trenberth KE, Fasullo JT, Kiehl J (2009) Earth's global energy budget. *Bull Am Meteorol Soc* 90(3):311–323. <https://doi.org/10.1175/2008BAMS2634.1>
- Voldoire A, Claudon M, Caniaux G et al (2014) Are atmospheric biases responsible for the tropical Atlantic SST biases in the CNRM-CM5 coupled model? *Clim Dyn* 43(11):2963–2984. <https://doi.org/10.1007/s00382-013-2036-x>
- Wahl S, Latif M, Park W et al (2011) On the tropical Atlantic SST warm bias in the Kiel climate model. *Clim Dyn* 36(5–6):891–906. <https://doi.org/10.1007/s00382-009-0690-9>
- Wang F, Chang P (2008) Coupled variability and predictability in a stochastic climate model of the tropical Atlantic. *J Clim* 21(23):6247–6259. <https://doi.org/10.1175/2008JCLI2283.1>
- Xie SP (2004) The shape of continents, air-sea interaction, and the rising branch of the Hadley circulation. In: Diaz HF, Bradley RS (eds) *The Hadley circulation: present, past and future*. Springer, Dordrecht, pp 121–152
- Xie P, Arkin PA (1997) Global precipitation: a 17-year monthly analysis based on gauge observations, satellite estimates, and numerical model outputs. *Bull Am Meteorol Soc* 78(11):2539–2558. [https://doi.org/10.1175/1520-0477\(1997\)078<2539:GPAYMA>2.0.CO;2](https://doi.org/10.1175/1520-0477(1997)078<2539:GPAYMA>2.0.CO;2)
- Xie SP, Carton JA (2004) Tropical Atlantic variability: patterns, mechanisms, and impacts. In: Wang C, Xie SP, Carton JA (eds) *Earth's climate: the ocean-atmosphere interaction*. American Geophysical Union, Washington, DC, pp 121–142. <https://doi.org/10.1029/147GM07>
- Xie SP, Philander SGH (1994) A coupled ocean-atmosphere model of relevance to the ITCZ in the eastern Pacific. *Tellus A* 46(4):340–350. <https://doi.org/10.1034/j.1600-0870.1994.t01-1-00001.x>
- Xu Z, Chang P, Richter I et al (2014) Diagnosing southeast tropical Atlantic SST and ocean circulation biases in the CMIP5 ensemble. *Clim Dyn* 43(11):3123–3145. <https://doi.org/10.1007/s00382-014-2247-9>
- Zebiak SE (1993) Air-sea interaction in the equatorial Atlantic region. *J Clim* 6(8):1567–1586
- Zermeño-Díaz DM, Zhang C (2013) Possible root causes of surface westerly biases over the equatorial Atlantic in global climate models. *J Clim* 26(20):8154–8168. <https://doi.org/10.1175/JCLI-D-12-00226.1>

Open Access This chapter is licensed under the terms of the Creative Commons Attribution 4.0 International License (<http://creativecommons.org/licenses/by/4.0/>), which permits use, sharing, adaptation, distribution and reproduction in any medium or format, as long as you give appropriate credit to the original author(s) and the source, provide a link to the Creative Commons license and indicate if changes were made.



The images or other third party material in this chapter are included in the chapter's Creative Commons license, unless indicated otherwise in a credit line to the material. If material is not included in the chapter's Creative Commons license and your intended use is not permitted by statutory regulation or exceeds the permitted use, you will need to obtain permission directly from the copyright holder.